ACS OMEGA

http://pubs.acs.org/journal/acsodf
Article

Copper(II) Complexes Derived from Halogen-Substituted Schiff Base Ligands: Synthesis, Crystal Structures, Antibacterial Activity, and Molecular Docking Studies

Published as part of ACS Omega special issue "3D Structures in Medicinal Chemistry and Chemical Biology".

Tunde Lewis Yusuf,* Ibrahim Waziri, Segun D. Oladipo, Mostafa S. Abd El-Maksoud, Alfred J. Muller, and Banele Vatsha*

Cite This: https://doi.org/10.1021/acsomega.4c06806

Read Online

ACCESS | Metrics & More | Article Recommendations | Supporting Information

ABSTRACT: In the face of escalating bacterial resistance to conventional antibiotics, the quest for novel antimicrobial strategies is urgenter than ever. Metal complexes, particularly those with biological activity, stand out as a promising alternative due to their unique mechanisms of action and potential for fewer side effects in comparison to standard organic antibiotics. This investigation focuses on the synthesis and characterization of six Cu(II) complexes, each formulated from halogen-substituted bidentate Schiff base ligands. Employing a suite of analytical methods, Fourier transform infrared, UV−vis, elemental analysis, and single-crystal X-ray diffraction, the structures of the complexes were fully established. All of the complexes were assigned to have square planar geometry, with the ligand acting as a bidentate and coordinate to the Cu(II) ion via nitrogen and oxygen atoms. The antibacterial efficacy of these complexes was rigorously tested against both Gram-positive bacteria *Staphylococcus aureus* and *Streptococcus pyogenes* and Gram-negative bacteria *Escherichia coli* and *Klebsiella pneumoniae*, utilizing the broth microdilution technique. The results revealed a spectrum of activity, with minimum inhibitory concentrations (MICs) spanning from less than 15.63 to 125 μg/mL. Notably, Complex **2** demonstrated remarkable potency against *S. aureus* and *S. pyogenes*, registering an MIC of less than 15.63 μg/mL. To elucidate the underlying mechanism of action, molecular docking studies were performed targeting the topoisomerase IV receptor. The docking outcomes corroborated the empirical data, underscoring the strong affinity of the complexes for the bacterial targets.

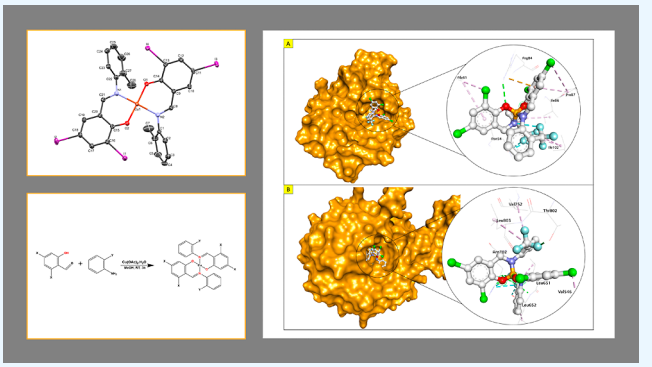

1. INTRODUCTION

The emergence and spread of bacterial antibiotic resistance have prompted intensive research efforts to identify new antimicrobial agents capable of addressing this growing surge.[1] While organic-based antimicrobial agents have been extensively studied, their efficacy has been compromised by the development of resistance mechanisms by bacteria. Thus, alternative strategies, such as metal-based antimicrobial agents, need to be explored, as they offer promising solutions in combating antibiotic-resistant bacteria.[2] Copper complexes have gained significant attention among metal-based antimicrobial agents due to their potent antimicrobial properties. Copper exhibits broad-spectrum activity and exerts its antimicrobial effects through multiple mechanisms, making it an attractive candidate for the development of novel antimicrobial agents. One approach to enhancing the antimicrobial activity of copper complexes is the utilization of halogen-substituted Schiff base ligands.[3,4] Halogen substitution in organic compounds has been widely explored in drug design and development due to the diverse chemical and biological properties imparted by halogens. In the context of antimicrobial agents, halogen-substituted compounds have shown enhanced activity against drug-resistant bacteria. The introduction of halogens, such as chlorine, bromine, or iodine, into the chemical structure of ligands, can modulate their physicochemical properties and improve their interaction with bacterial targets.[5] Schiff base ligands derived from halogen-substituted compounds have demonstrated great potential in metal complexation and antimicrobial activity. These ligands possess unique structural features that facilitate the formation

Received: July 24, 2024
Revised: October 4, 2024
Accepted: October 10, 2024

Scheme 1. Pathway for the Synthesis of the Complexes

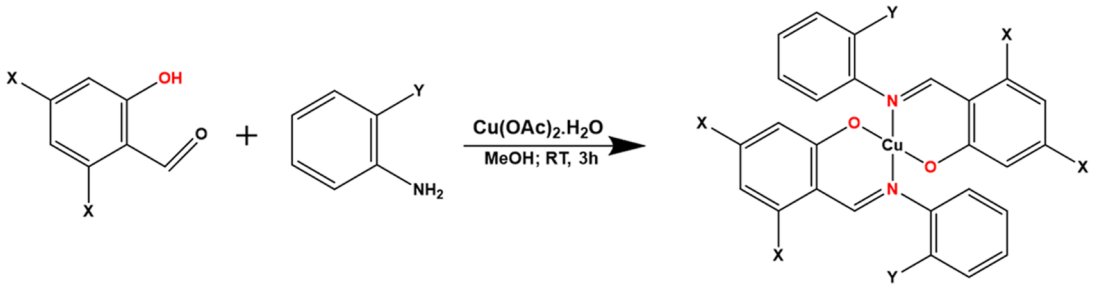

of stable and biologically active copper complexes. The resulting copper complexes derived from halogen-substituted Schiff base ligands have exhibited enhanced antimicrobial efficacy, making them promising candidates for addressing bacterial resistance to antibiotics.[6] Several studies have evaluated the antibacterial activity of copper complexes derived from Schiff base and halogen-substituted Schiff base ligands, demonstrating promising results. For example, El-Sawaf et al. (2023), synthesized a series of copper complexes derived from a Schiff base ligand and evaluated their antibacterial activity against Gram-positive and Gram-negative bacteria. The copper complexes exhibited potent antibacterial effects, including activity against multidrug-resistant strains.[7] In another study by Nazirkar et al. (2019), copper complexes derived from halogen-substituted Schiff base ligands were synthesized and assessed for their antimicrobial activity. The complexes demonstrated significant antibacterial effects against a range of clinically relevant bacterial strains including drug-resistant isolates. The researchers attributed the enhanced antimicrobial activity to the presence of halogen substituents, which increased the lipophilicity and antimicrobial properties of the complexes.[8] Furthermore, Guo et al. (2020) reported the synthesis and evaluation of copper complexes derived from a halogen-substituted Schiff base ligand against methicillin-resistant *Staphylococcus aureus* (MRSA). The copper complexes exhibited potent antibacterial activity, surpassing the activity of the parent organic compound. The researchers highlighted the role of halogen substitution in improving the antimicrobial properties of the copper complexes.[9] In a recent study by Joseph et al. (2017), a new series of copper complexes derived from halogen-substituted Schiff base ligands were synthesized and evaluated for their antibacterial activity. The copper complexes demonstrated excellent antimicrobial efficacy against both Gram-positive and Gram-negative bacteria including drug-resistant strains. The researchers attributed the enhanced activity to the presence of halogens, which facilitated improved interactions with bacterial targets.[10]

These studies exemplify the potential of copper complexes derived from Schiff base and halogen-substituted Schiff base ligands as effective antimicrobial agents. The incorporation of halogens into the ligands enhances the antimicrobial activity of the resulting copper complexes, making them viable candidates for combating antibiotic-resistant bacteria. The efficacy of halogen-substituted compounds in drug design and development has been well-established, exhibiting enhanced activity against drug-resistant bacteria. Therefore, this work reported the synthesis and antibacterial evaluation of copper complexes derived from halogen substituted Schiff base ligands.

2. EXPERIMENTAL SECTION

2.1. Chemicals and Instrumentation. Copper(II) acetate monohydrate, 2-chloroaniline, o-toluidine, 2-(trifluoromethyl)aniline, 3,5-dichlorosalicyaldehyde, 3,5-dibromosalicyaldehyde, and 3,5-diiodosalicyaldehyde were procured from Sigma-Aldrich. All solvents used in the study were purchased from Sigma-Aldrich, meeting ACS reagent grade standards (≥99.5%), and were utilized without further purification. Melting points (mp) were determined using the Electrothermal MEL-TEP 1002D apparatus and were reported without any corrections. Fourier transform infrared (FT-IR) spectra were acquired using a PerkinElmer Universal ATR spectrum 100 FT-IR spectrometer, covering the wavenumber range of 4000−400 cm^{-1}. Elemental analyses were conducted using a Thermal-Scientific Flash 2000 CHNS/O analyzer. Electronic absorption spectra were recorded on a Shimadzu UV-3600 UV−vis−NIR spectrophotometer, employing quartz cuvettes with a path length of 1 cm path length. The UV range covered 200−400 nm, while the visible range spanned 400−900 nm. High-resolution mass spectra (HRMS) were obtained by using a WatersAcquity UPLC Synapt G2 HD mass spectrometer.

2.2. Synthesis of the Complexes. The complexes **1**−**6** were synthesized using a one-pot in situ method without isolating the ligands. The synthesis procedures for the complexes were adapted from previously reported literature.[11] The specific details for the synthesis of each complex are as follows: A methanolic solution (1.0 mmol) of 3,5-dichlorosalicyaldehyde, 3,5-dibromosalicyaldehyde, 3,5-diiodosalicyaldehyde, or 3,5-dichlorobenzaldehyde was reacted with a methanolic solution (1.0 mmol) of primary amines, namely, 2-chloroaniline, o-toluidine, or 2-(trifluoromethyl)aniline at room temperature. This addition led to the formation of various colors in each mixture, which were stirred for 1 h. Subsequently, a solution of copper(II) acetate monohydrate (99.8 mg, 0.5 mmol) in 10 mL of methanol was added to each solution and stirred for 3 h. This addition resulted in the formation of a brown powder in all reactions. The brown powder was then filtered, washed with methanol under a vacuum, and allowed to dry before being transferred to a vial. The vial containing the brown powder was stored in a desiccator for further use. To grow crystals of each complex, vapor diffusion of hexane into a concentrated solution of dichloromethane was employed, yielding dark blue crystals for each of the complexes. The reaction pathway is shown in Scheme 1.

*2.2.1. Bis(E)-2,4-dichloro-6-(((2-chlorophenyl)imino)-methyl)phenolate copper(II) (**1**).* Brown solid; yield: 280 mg, 66.5%, mp: 246−248 °C; Anal. Calcd for $C_{26}H_{14}Cl_6CuN_2O_2$: C, 47.12; H, 2.13; N, 4.23. Found: C,

https://doi.org/10.1021/acsomega.4c06806
ACS Omega XXXX, XXX, XXX−XXX

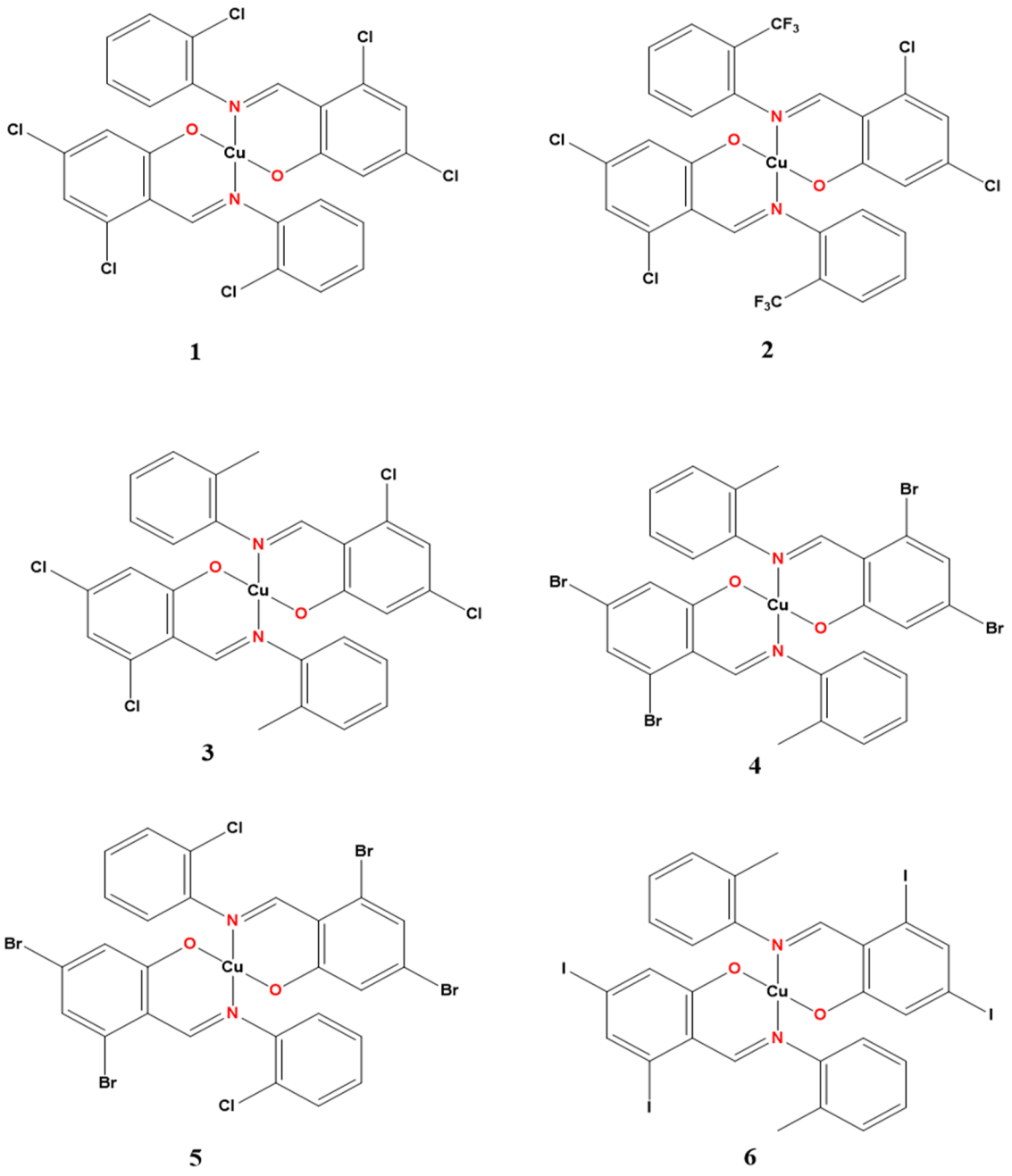

Figure 1. Structures of the complexes, **1**−**6**.

47.13; H, 2.13; N, 4.23; Selected IR data (ATR, cm^{-1}): 2681 (C−H), 1595 (C═N), 1315 (C−O), 751(C−Cl), 543 (Cu−N), 437 (Cu−O).

*2.2.2. Bis(E)-2,4-dichloro-6-(((2-(triflouromethyl)phenyl)-imino)methyl)phenolate copper(II) (**2**).* Brown solid; yield: 315 mg, 73.2%; mp: 236−238 °C; Anal. Calcd for: $C_{28}H_{14}Cl_4CuF_6N_2O_2$: C, 46.08; H, 1.93; N, 3.84. Found: C, 46.12; H, 1.99; N, 3.79; Selected IR data (ATR, cm^{-1}): 2953 (C−H), 1598 (C═N), 1400 (C−F), 1320 (C−O), 751 (C−Cl), 557 (Cu−N), 471 (Cu−O).

*2.2.3. Bis(E)-2,4-dichloro-6-((o-tolylimino)methyl)-phenolate copper(II) (**3**).* Pale brown; yield: 265 mg, 67.2%, mp: 239−241 °C; Anal. Calcd for: $C_{28}H_{20}Cl_4CuN_2O_2$: C, 54.08; H, 3.24; N, 4.51. Found: C, 54.03; H, 3.26; N, 4.55; Selected IR data (ATR, cm^{-1}): 2986 (C−H), 1602 (C═N), 1332 (C−O), 756 (C−Cl), 526 (Cu−N), 425 (Cu−O).

*2.2.4. Bis(E)-2,4-dibromo-6-((o-tolylimino)methyl)-phenolate copper(II) (**4**).* Dark brown solid; yield: 312 mg, 77.4%; mp: 237−239 °C; Anal. Calcd for: $C_{28}H_{20}Br_4CuN_2O_2$: C, 42.06; H, 2.52; N, 3.50. Found: C, 42.06; H, 2.59; N, 3.54; Selected IR data (ATR, cm^{-1}): 3008 (C−H), 1605 (C═N), 1323 (C−O), 670 (C−Br), 557 (Cu−N), 434 (Cu−O).

*2.2.5. Bis(E)-2,4-dibromo-6-(((2-chlorophenyl)imino)-methyl)phenolate copper(II) (**5**).* Brown solid; yield: 275 mm, 63.8%, mp: 250−251 °C; Anal. Calcd for: $C_{26}H_{14}Br_4Cl_2CuN_2O_2$: C, 37.16; H, 1.68; N, 3.33. Found: C, 37.09; H, 1.70; N, 3.25; Selected IR data (ATR, cm^{-1}): 3057 (C−H), 1590 (C═N), 1316 (C−O), 701 (C−Br), 536 (Cu−N), 420 (Cu−O).

*2.2.6. Bis(E)-2,4-diiodo-6-(((2-chlorophenyl)imino)-methyl)phenolate copper(II) (**6**).* Brown solid; yield: 288 mg, 58.6%, mp: 262−264 °C; Anal. Calcd for

https://doi.org/10.1021/acsomega.4c06806
ACS Omega XXXX, XXX, XXX−XXX

$C_{28}H_{20}CuI_4N_2O_2$: C, 34.05; H, 2.04; N, 2.84. Found: C, 34.07; H, 2.06; N, 2.82; Selected IR data (ATR, cm^{-1}): 3005 (C−H), 1600 (C═N), 1334 (C−O), 729 (C−I), 543 (Cu−N), 459 (Cu−O).

2.3. X-Ray Crystallography. A single crystal from **1−6** was selected from the mother liquor solution under a microscope and attached to a nylon loop by using Paratone-N oil. The loop with the crystal was then placed on a goniometer head under a nitrogen gas stream. Single-crystal X-ray diffraction data were acquired using MoKα radiation (λ = 0.71073 Å) on a Bruker DUO APEX II diffractometer. The diffractometer was equipped with a Bruker K780 generator operating at 45 kV and 30 mA. The intensity data were obtained and adjusted using the SAINT software.[12] Absorption correction of the collected intensities was performed using SADABS.[13] The structure was initially solved using SHELXS and then refined using SHELXL through the Olex2 software interface.[14] A graphical interface was created using X-SEED.[15]

2.4. In Vitro Antibacterial Study. The antimicrobial efficacy of complexes 1−6 was assessed against four bacterial strains, consisting of two Gram-positive and two Gram-negative bacteria. The Gram-positive strains included *S. aureus* (SA) (ATCC25923) and *Staphylococcus pyogenes* (SP) (ATCC19615), while the Gram-negative strains were *Escherichia coli* (EC) (ATCC25922) and *Klebsiella pneumoniae* (KP) (ATCC13882). The minimum inhibitory concentration (MIC) of the complexes was determined using the broth microdilution method, following the instructions outlined by.[16] To initiate the assay, 4 mg of each compound was accurately weighed and dissolved in 4 mL of dimethyl sulfoxide (DMSO). Subsequently, serial dilutions were performed six times to achieve the desired concentrations of 500, 250, 125, 62.5, 31.25, and 15.625 μg/mL. These dilutions were prepared in 100 μL of nutrient broth and dispensed into 96-well plates. Each concentration was duplicated, resulting in a total of 12 wells per compound. Next, 100 μL of an overnight bacterial culture, adjusted to a 0.5 McFarland standard in nutrient broth, was added to each well, effectively combining it with the compound solutions. The plates were then incubated overnight at 37 °C in a controlled environment using an incubator. To assess bacterial growth, resazurin dye was introduced into the wells, enabling the detection of viable cells based on their metabolic activity. For comparison and validation, positive controls such as ciprofloxacin and streptomycin were included, while the negative control consisted of 50% nutrient broth in DMSO. The MIC values, defined as the lowest concentration at which no visible growth was observed, were recorded for each complex against the respective bacterial strains.

2.5. Molecular Docking Study. The crystal structures of *E. coli*, *K. pneumoniae*, and *S. aureus* topoisomerases were obtained from the Protein Data Bank (PDB) with the following IDs: 1KZN, 5EIX, and 3TTZ, respectively. Additionally, the structure of *S. pyogenes* topoisomerase was modeled using AlphaFold (ID: AF-P0DG03-F1). To prepare the protein structures for docking studies, AutoDock Tools (ADT) was employed. This involved removing water and any bound ligands,[17] as well as adding missing atoms and polar hydrogens. The prepared protein structures were then converted to pdbqt files. The ligands' 3D structures were sketched and subjected to minimization using the Avogadro software.[18] For the docking studies, AutoDock Vina was utilized.[19] The resulting complexes were analyzed and visualized using Discovery Studio visualizer software.[20]

3. RESULTS AND DISCUSSION

3.1. Synthesis. The reaction pathway for synthesizing the Cu(II) derived halogen substituted ligands is shown in Scheme 1, and the structures of the complexes are presented in Figure 1. All of the complexes were obtained with a moderate yield (above 50%). The CHN-elemental analyses of the complexes presented data consistent with their structures. These results agree with those from X-ray crystallography. The solubility of the complexes in some selected polar and nonpolar solvents such as water, methanol, ethanol, chloroform, acetonitrile, dichloromethane, dimethyl sulfoxide, and dimethylformamide was tested, and the result showed the complexes are soluble in the tested solvents.

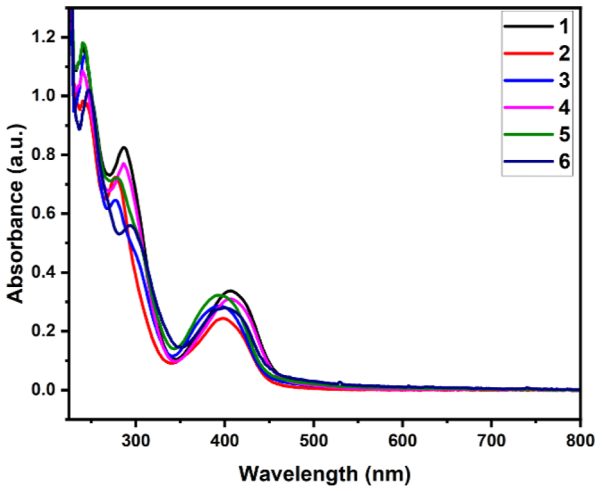

Figure 2. Electronic absorption spectra of the complexes.

3.2. Spectroscopy Studies of the Complexes. *3.2.1. UV−Visible Spectroscopy.* The electronic absorption spectra of the complexes 1−6 were obtained in dichloromethane in the range of 200−800 nm, and therein, two major absorption bands were observed, Figure 2. The first absorption band that appeared around 275−285 nm can be ascribed to the π—π^* transition due to the conjugated C═C chromophore present in the backbone ligand of the complexes. The second absorption band appeared around 385−395 nm and can be assigned to ligand-to-metal charge transfer (LMCT). An additional weak band was observed around 670−690 nm and was well pronounced when the concentration of the copper complexes was increased. This band can be assigned to the d—d transition ($^2E_g \rightarrow {}^2T_{2g}$).[21] All the observed bands in the spectra of 1−6 are related to the ones of Cu(II) Schiff base complexes previously reported.[22]

3.2.2. Fourier Transform Infrared Spectroscopy. The infrared absorption spectra of complexes **1−6** were obtained in the range of 4000−400 cm^{-1}, and the detailed spectra are presented in the Supporting Information. In all spectra, four major bands were observed, and these are ν(C−H), ν(C═N), ν(C−O), and ν(C−Cl, Br or I). In all the complexes, the ν(C−H) appeared around 3057−2681 cm^{-1}, respectively. The bands around 1605−1590 cm^{-1} and 1334−1315 cm^{-1} can be ascribed to the imine group (C═N) and ν(C−O). The values observed for these bands are comparable to those reported in the literature.[22] These two bands are diagnostic bands that affirm the coordination of phenolic oxygen and the imine group to the metal center in IR spectra. The bands for the

https://doi.org/10.1021/acsomega.4c06806
ACS Omega XXXX, XXX, XXX−XXX

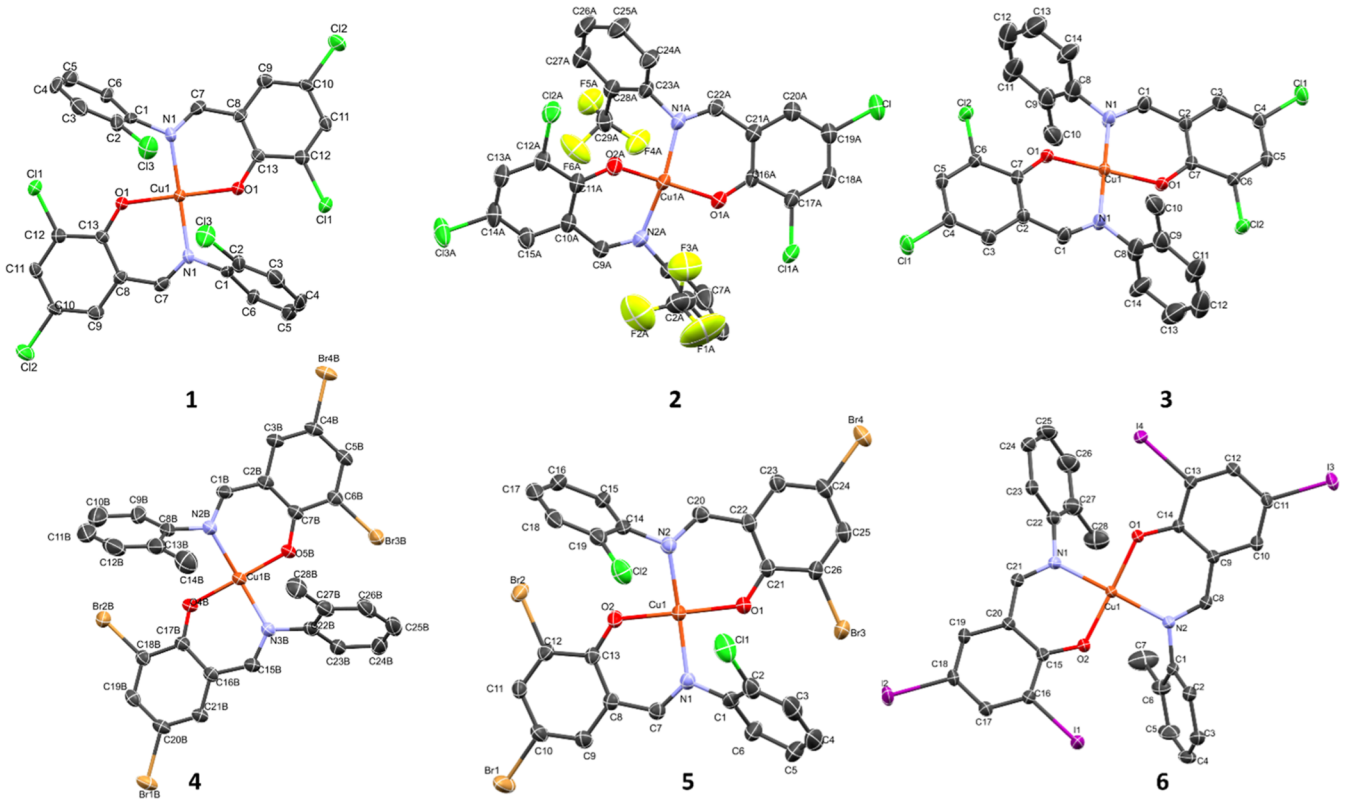

Figure 3. X-ray crystallographic representation of complexes **1**−**6**.

imine group shifted to a lower wavelength relative to the ligands and this confirms the complexation of nitrogen atom in ν(C═**N**) to the copper center.[23] The vibrational frequencies at 1334−1315 cm^{-1} is attributed to ν(C−O) and decreased by 3−10 cm^{-1} when compared to parent ligands. Other distinctive bands, such as ν(Cu−N) and ν(Cu−O), appeared around 557−420 cm^{-1}.

3.3. Description of the Crystal Structures. The single-crystal X-ray structures of the six copper Schiff base complexes were determined to elucidate their coordination geometry and intermolecular interactions. The single-crystal X-ray structures are presented in Figure 3. The crystallographic parameters for the six complexes, including unit cell dimensions, space group, and refinement details, are summarized in Table 1.

Each copper(II) center exhibits a square planar or slightly distorted square planar geometry. The coordination environment around the copper ion involves imine nitrogen (N) and phenolic oxygen (O) from the Schiff base ligand. The Cu−N bond lengths range from 1.90 to 2.02 Å, while the Cu−O bond lengths vary from 1.89 to 2.05 Å. The N−Cu−O bond angles are approximately 90°, reflecting the square planar geometry typically observed in such complexes and are consistent with typical copper(II) complexes.[4,22,24] All complexes are mononuclear, with complexes **2**, **4** and **5** consisting of two independent molecular units in the asymmetric unit, while complexes **1** and **3** showed only half of the molecular unit in the asymmetric unit. Complex **6** consists of one molecular unit of the complex and one solvate CH_2Cl_2 molecule in the asymmetric part of the unit cell. Further structural analysis revealed the presence of various intermolecular interactions. In Complex 6, the complex entities are linked through π−π stacking interactions, as evidenced by a centroid-to-centroid distance of 3.678 (3) Å. The complex is also stabilized in intermolecular bonding between C(18)−I(2)...C(2), C(18)−I(2)...C(2) and I4...I1 with distances of 3.539, 3.522, and 3.863 Å. Complex 1 is stabilized by Cl(2)...Cl(1) at a distance of 3.350 Å.

3.4. Antibacterial Study. The antimicrobial activities of the synthesized Cu(II) complexes were evaluated against two Gram-positive bacteria (*Staphylococcus pyogenes* and *S. aureus*) and two Gram-negative bacteria (*E. coli* and *K. pneumoniae*) using the broth microdilution method. The MIC values were compared to standard drugs (ciprofloxacin and ampicillin) following a standard protocol.[25]

The results, summarized in Table 2, showed that all of the complexes exhibited varying degrees of antimicrobial activity compared to the control. **2**, **3**, and **6** demonstrated broad-spectrum activity against both Gram-positive and Gram-negative strains. In contrast, **1**, **4**, and **5** displayed activities limited to Gram-positive strains only.

Specifically, 1 exhibited an MIC of 15.63 μg/mL on *S. aureus* and *Staphylococcus pyogenes*, and 31.25 μg/mL on *E. coli* and *K. pneumoniae*. **2** had an MIC below 15.63 μg/mL on Gram-positive strains and 15.63 μg/mL on Gram-negative strains. Complex **3** displayed an MIC of 15.63 μg/mL for all tested strains. Complex 4 exhibited an MIC of 62.5 μg/mL on *S. aureus* and *Staphylococcus pyogenes*, and 125 μg/mL on *E. coli* and *K. pneumoniae*. Complex **5** had an MIC of 31.25 μg/mL on Gram-positive strains and 62.5 μg/mL on Gram-negative strains. Similarly, complex **6** showed an MIC of 15.63 μg/mL for all tested bacteria.

The control drugs ciprofloxacin and ampicillin demonstrated respective MIC values of 15.63 μg/mL on Gram-positive strains and 31.25 μg/mL on Gram-negative strains.

Based on the results, chloro-substituted salicylaldehyde complexes demonstrated higher activity than their bromo

https://doi.org/10.1021/acsomega.4c06806
ACS Omega XXXX, XXX, XXX−XXX

Table 1. Selected Crystallographic and Structure Refinement Parameters for the Complexes 1−6

identification code	1	2	3	4	5	6.CH_2Cl_2
empirical formula	$C_{26}H_{14}Cl_6CuN_2O_2$	$C_{56}H_{28}Cl_8Cu_2F_{12}N_4O_4$	$C_{28}H_{20}Cl_4CuN_2O_2$	$C_{56}H_{40}Br_8Cu_2N_4O_4$	$C_{26}H_{14}Br_4Cl_2CuN_2O_2$	$C_{29}H_{22}Cl_2CuI_4N_2O_2$
formula weight	662.674	1457.426	621.839	1599.286	841.151	1072.579
temperature/K	172.80	173.00	173.00	173.00	173.00	173.00
crystal system	tetragonal	monoclinic	monoclinic	monoclinic	triclinic	monoclinic
space group	$P4_32_12$	$P2_1/n$	$P2_1/n$	$P2_1/n$	$P\bar{1}$	$C2/c$
a/Å	10.0930(4)	12.2170(4)	10.0975(5)	14.0013(3)	12.3038(4)	22.0638(7)
b/Å	10.0930(4)	28.8120(9)	10.1304(6)	21.9106(5)	13.9849(5)	12.7768(4)
c/Å	24.8776(17)	17.1436(7)	12.9854(7)	17.8400(4)	17.0121(6)	24.8432(11)
α/°	90	90	90	90	80.046(1)	90
β/°	90	110.762(1)	106.210(2)	93.288(1)	71.243(1)	110.403(1)
γ/°	90	90	90	90	75.396(1)	90
volume/Å^3	2534.2(2)	5642.6(4)	1275.49(12)	5463.9(2)	2668.72(16)	6564.0(4)
Z	4	4	2	4	4	8
ρ_{calc} g/cm^3	1.737	1.716	1.619	1.944	2.094	2.171
μ/mm^{-1}	1.525	1.224	1.306	6.679	7.037	4.620
F(000)	1329.6	2909.6	632.2	3094.0	1613.0	4002.3
crystal size/mm^3	0.147 × 0.094 × 0.041	0.168 × 0.1 × 0.035	0.19 × 0.113 × 0.037	0.341 × 0.183 × 0.029	0.233 × 0.118 × 0.041	0.14 × 0.108 × 0.031
radiation	Mo Kα (λ = 0.71073)	Mo Kα (λ = 0.71073)	Mo Kα (λ = 0.71073)	Mo Kα (λ = 0.71073)	Mo Kα (λ = 0.71073)	Mo Kα (λ = 0.71073)
2Θ range for data collection/°	4.36 to 55.7	2.82 to 55.84	5.18 to 55.8	3.46 to 55.8	2.54 to 55.84	3.5 to 55.8
index ranges	$-12 \le h \le 12$, $-5 \le k \le 13$, $-23 \le l \le 32$	$-16 \le h \le 16$, $-37 \le k \le 37$, $-22 \le l \le 22$	$-13 \le h \le 13$, $-13 \le k \le 13$, $-17 \le l \le 16$	$-17 \le h \le 18$, $-28 \le k \le 28$, $-23 \le l \le 22$	$-16 \le h \le 16$, $-18 \le k \le 18$, $-22 \le l \le 22$	$-28 \le h \le 28$, $-16 \le k \le 16$, $-32 \le l \le 32$
reflections collected	9623	87 370	20 961	83 300	117 552	172 042
independent reflections	2921 [R_{int} = 0.0856, R_{sigma} = 0.0885]	13 462 [R_{int} = 0.0876, R_{sigma} = 0.0611]	3039 [R_{int} = 0.0545, R_{sigma} = 0.0324]	12 944 [R_{int} = 0.0658, R_{sigma} = 0.0448]	12 738 [R_{int} = 0.0541, R_{sigma} = 0.0273]	7834 [R_{int} = 0.0481, R_{sigma} = 0.0143]
data/restraints/parameters	2921/0/168	13462/0/808	3039/1/170	12944/0/671	12738/0/732	7834/0/363
goodness-of-fit on F^2	1.037	1.047	1.040	1.036	1.055	1.048
final R indexes [$I \ge 2\sigma$ (I)]	R_1 = 0.0547, wR_2 = 0.1123	R_1 = 0.0582, wR_2 = 0.1201	R_1 = 0.0517, wR_2 = 0.1179	R_1 = 0.0317, wR_2 = 0.0646	R_1 = 0.0424, wR_2 = 0.0823	R_1 = 0.0259, wR_2 = 0.0602
final R indexes [all data]	R_1 = 0.0790, wR_2 = 0.1278	R_1 = 0.0956, wR_2 = 0.1431	R_1 = 0.0591, wR_2 = 0.1234	R_1 = 0.0514, wR_2 = 0.0714	R_1 = 0.0509, wR_2 = 0.0855	R_1 = 0.0304, wR_2 = 0.0636
largest diff. peak/hole/e Å^{-3}	1.20/−0.73	1.03/−0.87	1.40/−0.51	1.21/−0.75	1.78/−1.52	1.50/−1.36

https://doi.org/10.1021/acsomega.4c06806
ACS Omega XXXX, XXX, XXX−XXX

Table 2. Result of the Antibacterial Evaluation of the Complexes 1−6 on Some Selected Bacteria[a]

	MIC (μg/mL)			
	Gram-positive		Gram-negative	
entry	SA	SP	EC	KP
1	15.63	15.63	31.25	31.25
2	<15.63	<15.63	15.63	15.63
3	15.63	15.63	15.63	15.63
4	62.5	62.5	125	125
5	31.25	31.25	62.5	62.5
6	15.63	15.63	15.63	15.63
Cipro	15.63	15.63	31.25	31.25
Amp	31.25	31.25	31.25	31.25
DMSO	NA	NA	NA	NA

[a]SA = *Staphylococcus aureus*, SP = *Streptococcus pyogenes*, EC = *Escherichia coli*, KP = *Klebsiella pneumoniae*; Cipro = Ciprofloxacin, Amp = Ampicillin, NA = No activity. DMSO is included as negative control due to its usage as vehicle carrier for solubilization of the complexes.

Table 3. Activity Index of the Complexes Comparative to Ciprofloxacin against the Bacteria Strains

	activity index (%)			
entry	SA	SP	EC	KP
1	50	50	100	100
2	145	145	200	200
3	100	100	50	50
4	25	25	25	25
5	50	50	50	50
6	100	100	50	50

Table 4. Activity Index of the Complexes Comparative to Ampicillin against the Bacteria Strains

	activity index (%)			
entry	SA	SP	EC	KP
1	50	50	100	100
2	220	220	200	200
3	50	50	50	50
4	50	50	25	25
5	100	100	50	50
6	50	50	50	50

Table 5. Binding Energy (kcal\mol) of the Best-Docked Pose of the Complexes with the Studied Protein

	protein			
	S. aureus	*S. pyogenes*	*E. coli*	*K. pneumoniae*
compound	binding energy (kcal/mol)			
1	−7.8	−8.9	−7.5	−7.7
2	−8.5	−9.0	−7.8	−8.8
3	−8.1	−9.8	−7.6	−8.3
4	−7.5	−8.5	−7.3	−7.2
5	−7.4	−8.4	−7.3	−7.6
6	−7.8	−8.5	−7.2	−7.6

and iodo counterparts. Among the chloro-substituted complexes, **2**, which contained a $-CF_3$ moiety on the aniline ring, exhibited the highest viability, followed by complex **3**. The activity order among the chloro-substituted complexes was 2 > 3 > 1. Furthermore, the iodo-substituted complex 6 displayed higher activity than the bromo-substituted complexes 4 and 5. In general, complexes **2**, **3**, and **6** exhibited higher activity against the tested strains compared to the control drugs. One showed higher bacterial activity than ampicillin and similar activity to ciprofloxacin. Complex **5** displayed activity similar to that of ampicillin against Gram-positive strains but less activity than ciprofloxacin. Complex **4** exhibited the least viability among the tested bacteria at the concentrations used.

The presence of different halogen substituents (chloro, bromo, and iodo) on the Schiff base ligands contributes to variations in the electronic and steric properties of the complexes. In this case, the chloro-substituted complexes exhibited higher antibacterial activity than the bromo- and iodo-substituted complexes. Chlorine is an electron-withdrawing group, while bromine and iodine are less electron-withdrawing. The presence of electron-withdrawing chlorine atoms in the chloro-substituted complexes enhances their electron-deficient nature, which can strengthen the complexes' interaction with bacterial targets. This stronger interaction contributed to their higher antibacterial activity compared to the bromo- and iodo substituted complexes. In addition to this, Chlorine is less hydrophobic compared to bromine and iodine. The hydrophobicity of a compound can influence its solubility, membrane permeability, and interaction with the hydrophobic regions of bacterial cells. The chloro-substituted complexes, being less hydrophobic, will have better solubility and membrane permeability, allowing them to effectively reach their target sites within bacteria and exert their antibacterial effects. Similarly, iodine is larger in size compared to bromine and chlorine. The bulkier nature of the iodo-substituted complexes can affect their ability to interact with bacterial cells, as observed in complex **6**. Also, the presence of additional substituents on the aromatic rings in the complexes further affects their antibacterial activity. For example, complex **2**, which contained a CF_3 substituent on one aromatic ring and chlorine substituents, showed the highest activity. Similarly, Complex 3 exhibited significant antibacterial potency with methyl substituents on the other ring and chlorine substituents. These additional substituents modify the electronic properties and steric of the complexes, influencing their interaction with bacterial targets and enhancing their antibacterial effects.

3.4.1. Structure−Activity Relationship. The observed trend in antibacterial activity suggests a structure−activity relationship within the series of complexes. The presence of specific combinations of halogen and additional substituents leads to variations in the molecular structure and properties, which in turn affect the complexes' ability to interact with bacterial cells. This relationship explains why certain complexes displayed higher activity, while others showed lower or no activity against the tested bacterial strains.

3.4.2. Spectrum of Activity. The differences in the antibacterial activity against Gram-positive and Gram-negative bacteria can be attributed to variations in the cell wall structures and properties of these bacterial types. Complexes **2**, **6**, and **3** demonstrated activity against Gram-positive and Gram-negative bacteria, indicating their broad-spectrum antibacterial properties. On the other hand, complexes **1**, **4**, and **5**, which showed lower activity, were only effective against Gram-positive bacteria, suggesting a single spectrum of action.

3.4.3. Activity Index Analysis. The activity index in antimicrobial studies serves as a comparative metric to evaluate the potency of a compound relative to a standard drug or

https://doi.org/10.1021/acsomega.4c06806
ACS Omega XXXX, XXX, XXX−XXX

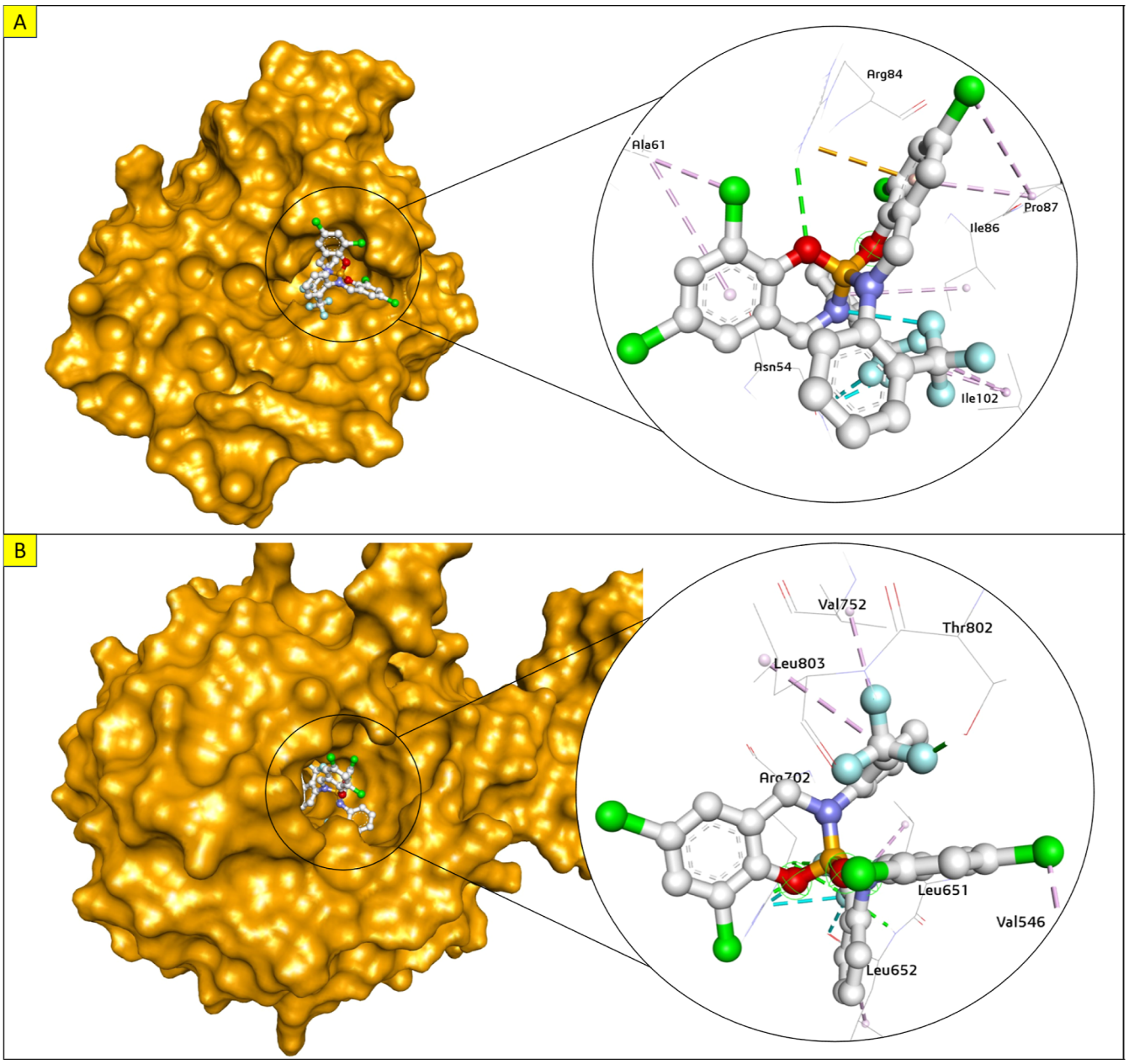

Figure 4. Surface mapping and 3D plot of complex **2** in the active site of (A) *S. aureus*. (B) *S. pyogenes*.

reference compound. It is calculated by comparing the effectiveness of the compound, often measured by parameters such as zone of inhibition or MIC, to that of the standard drug. This index provides a quantitative measure to assess the relative efficacy of new compounds in inhibiting microbial growth. Understanding the activity index is crucial in antimicrobial research as it helps in gauging the potential of novel compounds in combatting microbial infections, guiding the selection of promising candidates for further development, and potentially contributing to the discovery of new and more effective antimicrobial agents.

To estimate the % activity index for the synthesized complexes (**1**−**6**) and compare them to the standard drugs (Ciprofloxacin and Ampicillin) against the tested bacteria, the results of the MIC study were utilized.

The activity index of the complexes compared to those of ciprofloxacin and ampicillin against the tested bacterial strains is presented in Tables 3 and 4, respectively. This data illustrates the activity indices like the MIC. In comparison to ciprofloxacin, as presented in Table 3, Complex **1** shows an activity index of 50% on SA and SP, and 100% each on EC and KP. Meanwhile, Complex **2** exhibits 145% on SA and SP, and 200% on EC and KP. Similarly, Complex **3** demonstrates activity indices of 100% and 50% on SA and SP, and EC and KP, respectively. Complexes **4** and **5** have activity indices of 25% and 50% on all of the tested bacteria, respectively. However, Complex **6** displays an activity index of 100% on SA and SP, and 50% on EC and KP (Table 3). These results indicate that Complex **2** is the most potent among the complexes, with a potency exceeding that of ciprofloxacin.

Similarly, the activity index of the complexes compared with ampicillin is presented in Table 4. The results reveal that Complex **1** has an activity index of 50% on SA and SP, and 100% on EC and KP. Complex **2** shows an activity index of

https://doi.org/10.1021/acsomega.4c06806
ACS Omega XXXX, XXX, XXX−XXX

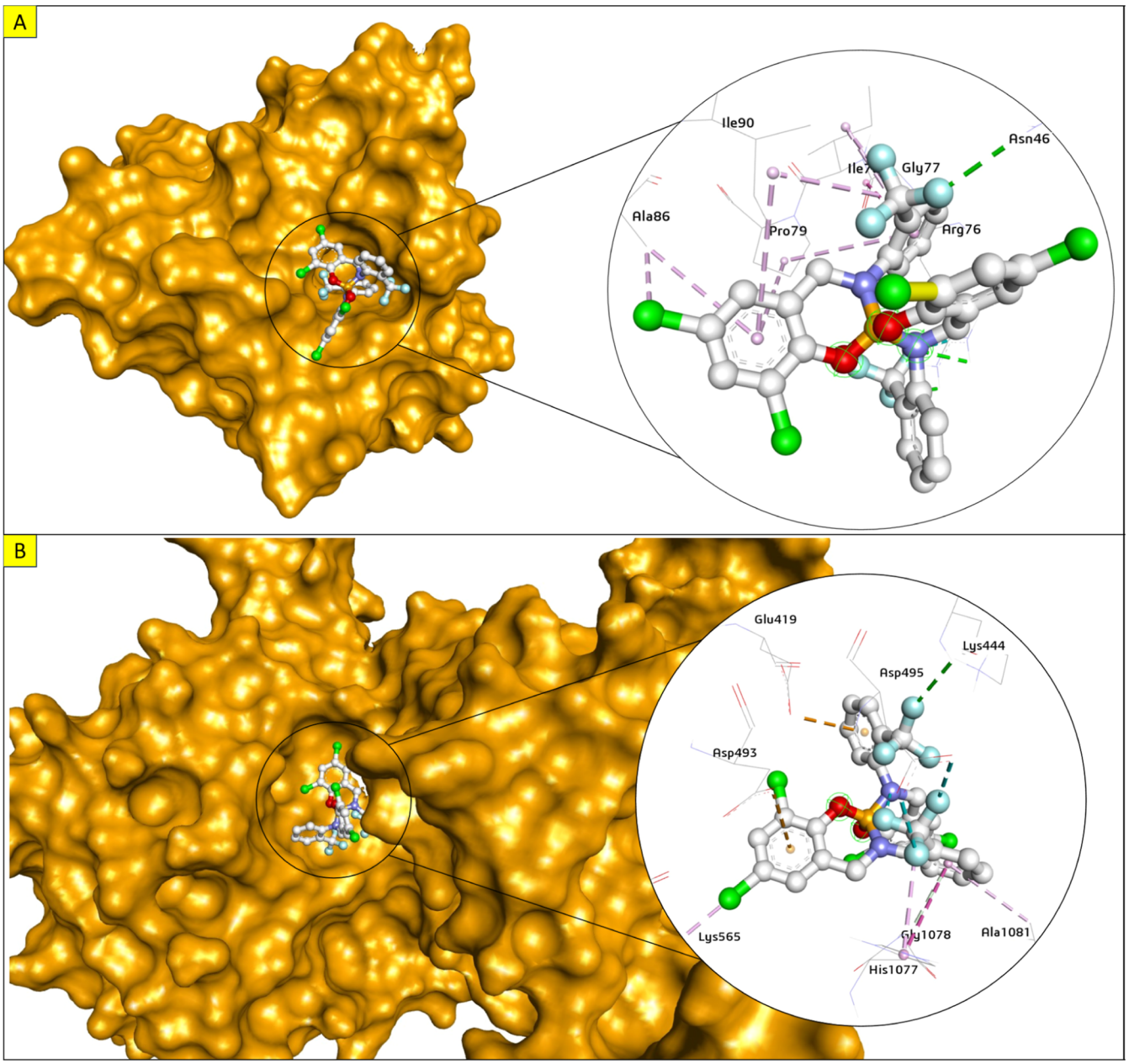

Figure 5. Surface mapping and 3D plot of complex **2** in the active site of (A) *E. coli* (B) *K. pneumoniae*.

220% on SA and SP, and 200% on EC and KP compared to ampicillin. Conversely, Complex **3** exhibits an activity index of 50% across all of the tested bacteria. Additionally, Complex **4** demonstrates activity indices of 50% and 25% on SA and SP, and EC and KP, respectively. Moreover, Complex **5** displays activity indices of 100% and 50% on SA and SP, and EC and KP, respectively. Furthermore, Complex **6** shows an activity index of 50% across all tested bacteria (Table 4). Overall, the complexes exhibit a similar trend in activity indices compared with the standard drug, with Complex **2** demonstrating superior activity in both cases.

3.5. Molecular Docking Study. Molecular docking was performed to investigate the binding mechanisms between our complexes and the target proteins. The binding scores of the ligand−protein interactions are presented in Table 5 below.

Based on the docking scores obtained, complex **2** exhibits the highest binding energy among the tested compounds. This result aligns well with the experimental data presented in Table 2, where complex 2 demonstrates the lowest MIC values. Therefore, complex **2** was chosen for further investigation to explore its mechanism of action against the targeted bacterial proteins. The interaction between the compound and receptors is illustrated in Figures 4, 5.

In Figure 4A, the binding interactions of complex **2** with the binding pocket of *S. aureus* topoisomerase are depicted. The compound forms a conventional hydrogen bond with the Arg84 residue. Additionally, the aromatic rings of the compound establish π bonds with the side chains of the Ala61, Ile86, Pro87, and Ile102 amino acids. The fluorine atoms interact with the Asn54 residue, and an π bond is formed between the cationic side chain of Arg84 and the aromatic ring of the compound. In addition, it exhibits efficient binding to *S. pyogenes* topoisomerase, with a binding score of −9.0 kcal/mol. In this case, it forms conventional hydrogen

https://doi.org/10.1021/acsomega.4c06806
ACS Omega XXXX, XXX, XXX−XXX

bonds with the Leu652, Arg702, Thr802, and Leu803 amino acids. π bonds are also observed with the side chains of the Val546, Leu651, and Val752 residues.

Figure 5A illustrates the binding of the compound with *E. coli* topoisomerase, where it forms conventional hydrogen bonds with Asn46 (2.56 Å) and Arg76 (2.65 and 2.88 Å) residues. The aromatic rings establish π bonds with the side chains of the Ile78, Pro79, Ala86, and Ile90 amino acids. Similarly, a π bond is formed with the amide group of the Gly77 amino acid. Furthermore, the compound interacts with *K. pneumoniae* topoisomerase, exhibiting a binding energy of −8.8 kcal/mol. It forms a strong conventional hydrogen bond with Lys444 (2.88 Å) and π−Alkyl bonds with the side chains of Lys565, His1077, and Ala1081 residues. π bonds are also observed with the anionic side chain of Glu419 and Asp493 residues. The fluorine atoms interact with Asp495, and an π−π bond is formed with His1077. Additionally, a C−H bond interaction is observed with Gly1078.

These binding interactions highlight the strong affinity of complex **2** toward the targeted topoisomerases, underscoring its potential as a promising led compound for further exploration in drug design and development.

4. CONCLUSION

In summary, we have successfully synthesized six new Cu(II) complexes using halogen-substituted Schiff base ligands through an in situ method. The complexes were thoroughly characterized using various physiochemical and spectroscopic techniques. Single crystal X-ray diffraction analysis confirmed the structures of all of the complexes, revealing a square planar and distorted square planar geometry in which the Cu(II) ion is coordinated by two phenolate oxygen atoms and two azomethine nitrogen atoms. To evaluate the antibacterial potential of the synthesized complexes, we conducted in vitro experiments using the broth dilution method. The results demonstrated varying degrees of antibacterial activity ranging from moderate to high. Notably, the chloro and iodo substituted complexes exhibited the most potent antibacterial effects, surpassing the activity of the standard control. Furthermore, we performed molecular docking studies of the led compound, complex **2**, using the topoisomerase IV receptor. The analysis revealed that hydrogen bonding, hydrophobic interactions, and π−π interactions are the main mechanisms of action between the compound and bacterial receptors. The promising antibacterial activity of the synthesized Cu(II) complexes, particularly the fluoro- and chloro-substituted variants, opens several avenues for further research. Evaluating these complexes against multidrug-resistant bacterial strains and assessing their potential for synergy with existing antibiotics could uncover new therapeutic strategies. Furthermore, in vivo studies are essential to determine pharmacokinetics, bioavailability, and toxicity, providing crucial data for advancing these complexes toward clinical applications.

■ ASSOCIATED CONTENT

Supporting Information

The Supporting Information is available free of charge at https://pubs.acs.org/doi/10.1021/acsomega.4c06806.

IR spectra of the complexes (PDF)

Combined cif_6m (CIF)

Accession Codes

CCDC 2272278−2272280, 2272284−2272285, and 2272287 contain supplementary crystallographic data for this paper. These data can be obtained free of charge from The Cambridge Crystallographic Data Centre via www.ccdc.cam.ac.uk/structures

■ AUTHOR INFORMATION

Corresponding Authors

Tunde Lewis Yusuf − *Department of Chemistry, Faculty of Natural and Agricultural Sciences, University of Pretoria, Pretoria 0028, South Africa;* orcid.org/0000-0003-3419-9516; Email: yusuf.tl@up.ac.za

Banele Vatsha − *Department of Chemical Sciences, University of Johannesburg, Johannesburg 2006, South Africa;* orcid.org/0000-0002-1420-1087; Email: vatsha@uj.ac.za

Authors

Ibrahim Waziri − *Department of Chemical Sciences, University of Johannesburg, Johannesburg 2006, South Africa;* orcid.org/0000-0003-0995-0451

Segun D. Oladipo − *Department of Chemical Sciences, Olabisi Onabanjo University, Ago-Iwoye, P. M. B 2002, Nigeria; Department of Chemistry and Polymer Science, Stellenbosch University, Matieland 7602, South Africa*

Mostafa S. Abd El-Maksoud − *Department of Pharmacology and Toxicology, Al-Azhar University, Assiut Branch, Assiut 71524, Egypt*

Alfred J. Muller − *Department of Chemical Sciences, University of Johannesburg, Johannesburg 2006, South Africa;* orcid.org/0000-0003-2304-6987

Complete contact information is available at: https://pubs.acs.org/10.1021/acsomega.4c06806

Author Contributions

The study was conceived and designed collaboratively by all authors. They collectively acquired the data, conducted the analysis, and interpreted the results. The manuscript was drafted and critically revised by all authors, ensuring the inclusion of significant intellectual content. Final approval for the publication of the manuscript was provided by all authors.

Notes

The authors declare no competing financial interest.

■ ACKNOWLEDGMENTS

The author would also like to thank the University of Johannesburg and the University of Pretoria for providing the necessary resources and infrastructure for the research. I.W. is grateful to the University Research Centre (URC) at the University of Johannesburg for awarding the postdoctoral research fellowship.

■ REFERENCES

(1) (a) Waziri, I.; Isa, M. A.; Sonopo, M.; Williams, D. B. G.; Muller, A. Synthesis, anti-microbial, toxicity and molecular docking studies of N-nitroso-N-phenylhydroxylamine (Cupferron) and its derivatives. *Bioorg. Med. Chem. Lett.* **2021**, *52*, 128381. (b) Prestinaci, F.; Pezzotti, P.; Pantosti, A. Antimicrobial resistance: a global multifaceted phenomenon. *Pathog. Global Health* **2015**, *109* (7), 309−318. (c) Salam, M. A.Al-Amin, M. Y.Salam, M. T.Pawar, J. S.Akhter, N.Rabaan, A. A.Alqumber, M. A.Antimicrobial resistance: a growing serious threat for global public health*Healthcare*; MDPI, 2023*11*1946

(2) (a) Fan, D.; Liu, X.; Ren, Y.; Bai, S.; Li, Y.; Luo, Z.; Dong, J.; Chen, F.; Zeng, W. Functional insights to the development of bioactive material for combating bacterial infections. *Front. Bioeng. Biotechnol.* **2023**, *11*, 1186637. (b) Xuan, J.; Feng, W.; Wang, J.; Wang, R.; Zhang, B.; Bo, L.; Chen, Z.-S.; Yang, H.; Sun, L. Antimicrobial peptides for combating drug-resistant bacterial infections. *Drug Resistance Updates* **2023**, *68*, 100954. (c) Muteeb, G.; Rehman, M. T.; Shahwan, M.; Aatif, M. Origin of antibiotics and antibiotic resistance, and their impacts on drug development: A narrative review. *Pharmaceuticals* **2023**, *16* (11), 1615.

(3) (a) Evans, A.; Kavanagh, K. A. Evaluation of metal-based antimicrobial compounds for the treatment of bacterial pathogens. *J. Med. Microbiol.* **2021**, *70* (5), 001363. (b) Frei, A.; Verderosa, A. D.; Elliott, A. G.; Zuegg, J.; Blaskovich, M. A. Metals to combat antimicrobial resistance. *Nat. Rev. Chem* **2023**, *7* (3), 202−224. (c) Waziri, I.; Masena, H. M.; Yusuf, T. L.; Coetzee, L.-C. C.; Adeyinka, A. S.; Muller, A. J. Synthesis, characterization, biological evaluation, DFT and molecular docking studies of (Z)-2-(((2-bromo-4-chlorophenyl) imino) methyl)-4-chlorophenol and its Co (ii), Ni (ii), Cu (ii), and Zn (ii) complexes. *New J. Chem.* **2023**, *47* (38), 17853−17870. (d) Yusuf, T. L.; Oladipo, S. D.; Zamisa, S.; Kumalo, H. M.; Lawal, I. A.; Lawal, M. M.; Mabuba, N. Design of new Schiff-Base Copper (II) complexes: Synthesis, crystal structures, DFT study, and binding potency toward cytochrome P450 3A4. *ACS Omega* **2021**, *6* (21), 13704−13718.

(4) Yusuf, T. L.; Waziri, I.; Olofinsan, K. A.; Akintemi, E. O.; Hosten, E. C.; Muller, A. J. Evaluating the in vitro antidiabetic, antibacterial and antioxidant properties of copper (II) Schiff base complexes: An experimental and computational studies. *J. Mol. Liq.* **2023**, *389*, 122845.

(5) (a) Waziri, I.; Yusuf, T. L.; Akintemi, E.; Kelani, M. T.; Muller, A. Spectroscopic, crystal structure, antimicrobial and antioxidant evaluations of new Schiff base compounds: An experimental and theoretical study. *J. Mol. Struct.* **2023**, *1273*, 134382. (b) Waziri, I.; Kelani, M. T.; Oyedeji-Amusa, M. O.; Oyebamiji, A. K.; Coetzee, L.-C. C.; Adeyinka, A. S.; Muller, A. J. Synthesis and computational investigation of N, N-dimethyl-4-[(Z)-(phenylimino) methyl] aniline derivatives: Biological and quantitative structural activity relationship studies. *J. Mol. Struct.* **2023**, *1276*, 134756. (c) Waziri, I.; Yusuf, T. L.; Zarma, H. A.; Oselusi, S. O.; Coetzee, L.-C. C.; Adeyinka, A. S. New palladium (II) complexes from halogen substituted Schiff base ligands: Synthesis, spectroscopic, biological activity, density functional theory, and molecular docking investigations. *Inorg. Chim. Acta* **2023**, *552*, 121505.

(6) (a) Elsamra, R. M.; Masoud, M. S.; Ramadan, A. M. Designing metal chelates of halogenated sulfonamide Schiff bases as potent nonplatinum anticancer drugs using spectroscopic, molecular docking and biological studies. *Sci. Rep.* **2022**, *12* (1), 20192. (b) More, M.; Joshi, P.; Mishra, Y.; Khanna, P. Metal complexes driven from Schiff bases and semicarbazones for biomedical and allied applications: a review. *Mater. Today Chem.* **2019**, *14*, 100195. (c) Venkatesh, G.; Vennila, P.; Kaya, S.; Ahmed, S. B.; Sumathi, P.; Siva, V.; Rajendran, P.; Kamal, C. Synthesis and Spectroscopic Characterization of Schiff Base Metal Complexes, Biological Activity, and Molecular Docking Studies. *ACS Omega* **2024**, *9*, 8123.

(7) El-Sawaf, A. K.; Madkour, M.; El-Samanody, E.-S. A. Synthesis, spectroscopic characterization, molecular studies, and biological evaluation of (E)-N'-((7-methyl-2-oxo-1, 2-dihydroquinolin-3-yl) methylene) morpholine-4-carbothiohydrazide and some of its transition metal complexes. *Inorg. Chim. Acta* **2023**, *554*, 121558.

(8) Nazirkar, B.; Mandewale, M.; Yamgar, R. Synthesis, characterization and antibacterial activity of Cu (II) and Zn (II) complexes of 5-aminobenzofuran-2-carboxylate Schiff base ligands. *J. Taibah Univ. Sci.* **2019**, *13* (1), 440−449.

(9) Guo, Y.; Hu, X.; Zhang, X.; Pu, X.; Wang, Y. The synthesis of a Cu (ii) Schiff base complex using a bidentate N 2 O 2 donor ligand: crystal structure, photophysical properties, and antibacterial activities. *RSC Adv.* **2019**, *9* (71), 41737−41744.

(10) Joseph, J.; Suman, A.; Nagashri, K.; Joseyphus, R. S.; Balakrishnan, N. Synthesis, characterization and biological studies of copper (II) complexes with 2-aminobenzimidazole derivatives. *J. Mol. Struct.* **2017**, *1137*, 17−26.

(11) Dehkhodaei, M.; Khorshidifard, M.; Rudbari, H. A.; Sahihi, M.; Azimi, G.; Habibi, N.; Taheri, S.; Bruno, G.; Azadbakht, R. Synthesis, characterization, crystal structure and DNA, HSA-binding studies of four Schiff base complexes derived from salicylaldehyde and isopropylamine. *Inorg. Chim. Acta* **2017**, *466*, 48−60.

(12) Saint, N. *Version 6.45*; Bruker Analytical X-ray Systems. Inc.: Madison, WI, 2003.

(13) Sheldrick, G.; Sadabs, A. *Software for Empirical Absorption Correction*; Version 2.05; University of Göttingen: Göttingen, Germany, 2002.

(14) Sheldrick, G. M. Program for crystal structure solution and refinement. In *SHELXS-97 and SHELXL-97*; University of Gottingen, 1997.

(15) Barbour, L. J. X-Seed 4: updates to a program for small-molecule supramolecular crystallography. *J. Appl. Crystallogr.* **2020**, *53* (4), 1141−1146.

(16) (a) Wiegand, I.; Hilpert, K.; Hancock, R. E. Agar and broth dilution methods to determine the minimal inhibitory concentration (MIC) of antimicrobial substances. *Nat. Protoc.* **2008**, *3* (2), 163−175. (b) Kowalska-Krochmal, B.; Dudek-Wicher, R. The Minimum Inhibitory Concentration of Antibiotics: Methods, Interpretation, Clinical Relevance. *Pathogens* **2021**, *10*, 165 . Note: MDPI stays neutral with regard to jurisdictional claims in published: 2021.

(17) Morris, G. M.; Huey, R.; Lindstrom, W.; Sanner, M. F.; Belew, R. K.; Goodsell, D. S.; Olson, A. J. AutoDock4 and AutoDockTools4: Automated docking with selective receptor flexibility. *J. Comput. Chem.* **2009**, *30* (16), 2785−2791.

(18) Hanwell, M. D.; Curtis, D. E.; Lonie, D. C.; Vandermeersch, T.; Zurek, E.; Hutchison, G. R. Avogadro: an advanced semantic chemical editor, visualization, and analysis platform. *J. Cheminf.* **2012**, *4*, 17.

(19) Trott, O.; Olson, A. J. AutoDock Vina: improving the speed and accuracy of docking with a new scoring function, efficient optimization, and multithreading. *J. Comput. Chem.* **2010**, *31* (2), 455−461.

(20) Dsjsd, B. *Discovery Studio Modeling Environment Release 2017*; Dassault Systemes, 2016; p 318.

(21) Hazra, M.; Dolai, T.; Pandey, A.; Dey, S. K.; Patra, A. Synthesis and characterisation of copper (II) complexes with tridentate NNO functionalized ligand: Density function theory study, DNA binding mechanism, optical properties, and biological application. *Inorg. Chem. Appl.* **2014**, *2014*, 1−13.

(22) (a) Yusuf, T. L.; Akintayo, D. C.; Oladipo, S. D.; Adeleke, A. A.; Olofinsan, K.; Vatsha, B.; Mabuba, N. J. N. J. o. C. The effect of structural configuration on the DNA binding and in vitro antioxidant properties of new copper (ii) N 2 O 2 Schiff base complexes. *New J. Chem.* **2022**, *46* (27), 12968−12980. (b) Yusuf, T. L.; Oladipo, S. D.; Zamisa, S.; Kumalo, H. M.; Lawal, I. A.; Lawal, M. M.; Mabuba, N. J. A. o. Design of new Schiff-Base Copper (II) complexes: Synthesis, crystal structures, DFT study, and binding potency toward cytochrome P450 3A4. *ACS Omega* **2021**, *6* (21), 13704−13718.

(23) Yusuf, T. L.; Oladipo, S. D.; Olagboye, S. A.; Zamisa, S. J.; Tolufashe, G. F. J. J. o. M. S. Solvent-free synthesis of nitrobenzyl Schiff bases: Characterization, antibacterial studies, density functional theory and molecular docking studies. *J. Mol. Struct.* **2020**, *1222*, 128857.

(24) Olagboye, S. A.; Yusuf, T. L.; Oladipo, S. D.; Zamisa, S. J. Crystal structure of bis (2-hydroxy-6-((phenylimino) methyl) phenolato-κ2N, O) copper (II), C26H20CuN2O4. *Z. Kristallogr. - New Cryst. Struct.* **2020**, *235* (3), 689−692.

(25) Hasselmann, C. Determination of minimum inhibitory concentrations (MICs) of antibacterial agents by broth dilution. *Clin. Microbiol. Infect.* **2003**, *9*(8), 9−15.

https://doi.org/10.1021/acsomega.4c06806
ACS Omega XXXX, XXX, XXX−XXX